The motion of rotating cylinders sliding on pebbled ice

Mark R.A. Shegelski, Matthew Reid, and Ross Niebergall

Abstract: We consider the motion of a cylinder with the same mass and size as a curling rock, but with a very different contact geometry. Whereas the contact area of a curling rock is a thin annulus having a radius of 6.25 cm and width of about 4 mm, the contact area of the cylinder investigated takes the form of several linear segments regularly spaced around the outer edge of the cylinder, directed radially outward from the center, with length 2 cm and width 4 mm. We consider the motion of this cylinder as it rotates and slides over ice having the nature of the ice surface used in the sport of curling. We have previously presented a physical model that accounts for the motion of curling rocks; we extend this model to explain the motion of the cylinder under investigation. In particular, we focus on slow rotation, i.e., the rotational speed of the contact areas of the cylinder about the center of mass is small compared to the translational speed of the center of mass. The principal features of the model are *(i)* that the kinetic friction induces melting of the ice, with the consequence that there exists a thin film of liquid water lying between the contact areas of the cylinder and the ice; *(ii)* that the radial segments drag some of the thin liquid film around the cylinder as it rotates, with the consequence that the relative velocity between the cylinder and the thin liquid film is significantly different than the relative velocity between the cylinder and the underlying solid ice surface. Since it is the former relative velocity that dictates the nature of the motion of the cylinder, our model predicts, and observations confirm, that such a slowly rotating cylinder *stops rotating well before translational motion ceases.* This is in sharp contrast to the usual case of most slowly rotating cylinders, where both rotational and translational motion cease at the same instant. We have verified this prediction of our model by careful comparison to the actual motion of a cylinder having a contact area as described.

PACS Nos.: 46.00, 01.80+b

Résumé: Nous étudions le mouvement d'un cylindre de masse et de grosseur égales à celles d'une pierre de curling, mais avec une géométrie de surface de contact très différente. Là où la surface de contact d'une pierre de curling est un anneau mince de rayon d'environ 6,25 cm et de largeur d'environ 4 mm, la surface de contact de notre cylindre prend la forme de plusieurs segments linéaires régulièrement espacés autour de la bordure extérieure du cylindre, dirigés radialement à partir du centre avec une longueur de 2 cm et une largeur de 4 mm. Nous étudions le mouvement de ce cylindre lorsqu'il tourne et glisse sur une surface glacée semblable à celle utilisée pour jouer au curling. Nous avons précédemment proposé un modèle physique pour décrire le mouvement de la pierre de curling. Nous étendons ce modèle pour décrire le cylindre décrit ci-dessus. Nous nous limitons aux rotations lentes, i.e., la vitesse tangentielle des surfaces de contact du cylindre en rotation autour du C.M. est petite par rapport à la vitesse de

Received August 6, 1999. Accepted December 1, 1999.

M.R.A. Shegelski[1] **and M. Reid.** Department of Physics, University of Northern British Columbia, 3333 University Way, Prince George, BC V2N 4Z9, Canada.
R. Niebergall. Department of Mathematics and Computer Science, University of Northern British Columbia, 3333 University Way, Prince George, BC V2N 4Z9, Canada.

[1] Corresponding author: **Telephone:** (250) 960–6663; **FAX:** (250) 960–5545; **e-mail:** mras@unbc.ca

translation du C.M. Les caractéristiques principales du modèle sont : *(i)* que la friction cinétique fond la glace, créant un film d'eau liquide entre la surface de contact du cylindre et la glace; *(ii)* que les segments radiaux transportent une partie du film d'eau autour du cylindre lorsqu'il tourne, la conséquence étant que la vitesse relative entre le cylindre et le film est notablement plus faible qu'entre le cylindre et la glace. Puisque c'est la première qui détermine la nature du mouvement du cylindre, notre modèle prédit et l'observation le confirme, qu'un tel cylindre en rotation cesse de tourner longtemps avant que ne cesse son mouvement de translation. Ceci contraste nettement avec le cas du cylindre à fond plat où rotation et translation cessent en même temps. Nous avons vérifié cette prédiction de notre modèle en observant le mouvement réel d'un cylindre construit tel que décrit ici.
[Traduit par la rédaction]

1. Introduction

In previous works [1,2], we investigated the motion of slowly and rapidly rotating curling rocks. The model we developed successfully accounts for a wide range of observed behaviour. In particular, the model explains the rather novel motion exhibited by curling rocks that are rotating rapidly and moving slowly translationally, specifically that the translational motion ceases well before the rotational motion. For almost all cases of rotating cylinders sliding over smooth, solid surfaces, the rotational and translational motion cease at the same instant.

The primary purpose of this paper is to investigate the possibility of rotation stopping prior to translational motion. Our model predicts that, if the contact area of the cylinder has a particular geometry (to be specified below), such motion should be observed. To understand what the contact geometry should be, it is necessary to first briefly review the principal features of our model, and how the model accounts for the observed motion of a rapidly rotating curling rock, and also some basic aspects of curling rocks and the surface of the ice sheet in the sport of curling.

We will then extend our model to the case of slowly rotating cylinders having the particular contact geometry referred to above. We will focus on the case of slowly rotating cylinders, and will explain why this is of most interest. By slow rotation, we simply mean that the speed with which the contact areas rotate about the center of mass is small compared to the translational speed of the center of mass. We explain the hypothesis and assumptions needed for the treatment of slow rotation. We then present the equations that describe the motion of a slowly rotating cylinder. The equations are solved both analytically and numerically to obtain the development in time of the cylinder's translational and rotational speeds. The results are compared to observed motions of slowly rotating cylinders.

2. The observed motion of curling rocks

In the sport of curling, cylindrical granite rocks slide over pebbled ice. Only a brief account of the aspects of curling most relevant to this paper will be conveyed here. More details are given in our previous paper [1].

The two principal aspects of curling relevant to this paper are the shape of the bottom of a curling rock, and the nature of "pebbled" ice.

Curling rocks have a small contact area with the ice: the bottom of the rock is hollowed and curved. Only a thin annulus of radius $r \approx 6.25$ cm and width $\Delta r \approx 3$ to 5 mm makes contact with the ice. Moreover, the sheet of ice is *not* flat. Instead, the surface of curling ice consists of many rounded protrusions with accompanying hollows, and is referred to as "pebbled ice". One consequence of the nature of the ice surface is that only a fraction of the annulus of the curling rock makes contact with the ice. This results in higher pressure exerted on the ice by the rock. The pressure results in kinetic melting of the ice as the rock passes over it. (This melting is *not* due to the pressure *directly*, but instead occurs because of the relative motion between the rock and the ice.)

A curling rock projected along a sheet of curling ice, with a small initial rotation, travels in a curved path. This is drastically different than, for example, the path of a hockey puck over the surface of hockey

ice. The curling rock moves laterally, across the sheet of ice, as it moves down the ice, whereas the hockey puck moves in a straight line. The lateral motion of a curling rock is novel in other ways as well. For example, a cylindrical, symmetrical, overturned drinking glass, projected over a smooth surface, and given an initial rotation, will also exhibit lateral motion (this is easily understood as a consequence of the nonuniform normal force [3]). One interesting aspect of curling rock motion is that curling rocks curl *in the direction opposite* to that of, for example, an overturned drinking glass.

In previous works [1,2], we developed a model that accounts for the observed motion of curling rocks. We first addressed the case of slow rotation because almost all the curling shots made by competent, knowledgeable curlers have $r\omega_0 << v_0$, where ω_0 is the initial angular speed, v_0 is the initial translational speed of the center of mass of the rock, and r is the radius of the contact annulus of the rock.

One of the principal features of our model is the idea that the motion of the rock over the ice results in melting of the ice and the formation of a thin film of liquid water. The adhesive force between the granite and the liquid water will accelerate some of the liquid and thereby drag it along with the rock as it rotates. This proved to be a chief feature in our explanation of why a curling rock curls, especially in the latter stages of the motion. Specifically, the adhesion between the rock and the liquid film drags some of the liquid to the front of the rock. The consequence is that the *front* portion of the contact annulus experiences mostly *wet* friction, and the *back* experiences mostly *dry* friction. The front of the rock is thus subjected to less friction than the back. Consequently, a curling rock, rotating slowly counterclockwise, curls to the left as viewed from above. (For complete details, see ref. 1.)

In a recent work [2], we extended our model to the case of rapidly rotating curling rocks. The main idea in this case is that the adhesive force between the granite and the liquid film results in some of the liquid being drawn around the rock, with the consequence that the relative velocity between the contact annulus and the portion of the liquid film in contact with the granite will be considerably different from the relative velocity between the contact annulus and the solid ice surface; the reason is that the liquid tends to circle around the annulus, and is thus moving relative to the solid ice surface. The force exerted on a given portion of the contact annulus of the rock, is therefore not in the direction opposite to the relative motion of the portion of the rock with respect to the solid ice surface, but is, instead, in the direction opposite to the direction of motion of the portion of the rock relative to the adjacent liquid film. Consequently, the torque on the rock is substantially reduced while the force is not. The result is that the rotational speed drops much more slowly than the translational speed, and translational motion ceases prior to rotational motion.

3. Theory of the motion of slowly rotating cylinders

We extend these ideas and our model to the case of slowly rotating cylinders sliding over pebbled ice. Our objective is to study a contact geometry, the nature of which is such that the cylinder will stop rotating before it ceases its translational motion, i.e., the opposite of what happens for rapidly rotating curling rocks.

It is the dragging of the thin liquid film around the contact annulus that is the fundamental physical reason for the behaviour of rapidly rotating curling rocks. This motion of the liquid is tangential to the contact annulus, and thus also tangential to a vector from the center of the contact annulus to a point on the contact annulus.

We make the following hypothesis. Suppose we replace the contact annulus by thin linear segments that are directed radially outward from the center of the rock, as depicted in Fig. 1. We hypothesize that the adhesion between the contact segments and the liquid film will be such that the liquid will be dragged primarily *along the length* of the contact segment, i.e., radially outward from, or inward toward, the center of the bottom of the cylinder, and almost not at all *perpendicular* to the segment, i.e., perpendicular to the radial direction. If, while rotating and sliding over the pebbled ice surface, these radial segments do indeed drag some of the liquid film radially along the segments, we will have,

Fig. 1. The contact area of the cylinder consists of rectangular segments with the longer sides oriented radially away from the center. In the case of the cylinder studied in this paper, the total area of these contact segments is about the same as the contact area of the contact annulus of a curling rock. We chose to manufacture a contact geometry consisting of 20 such segments, each 2 cm long and 4 mm wide. Note also the radius r of the plate under which the segments were fastened, as well as the radius R of the curling rock that was placed on top of the plate. Note that $r > R$; $R = 0.14$ m, and we chose $r = 0.20$ m (see text for details). Note that the figure is not drawn to scale.

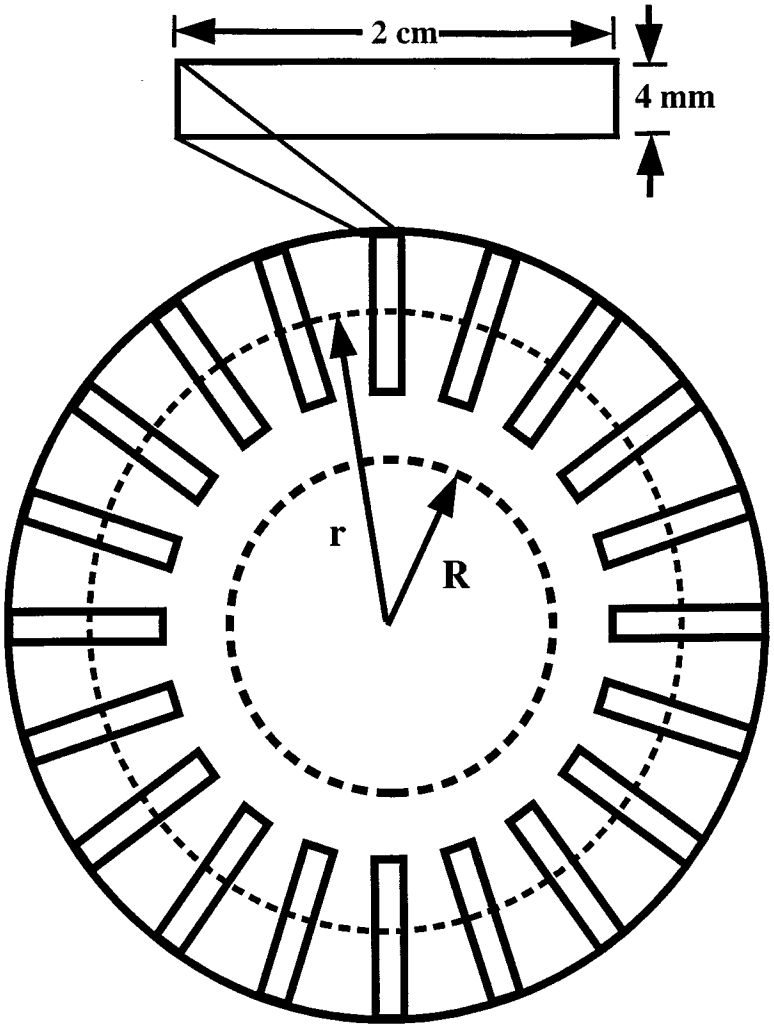

as we did before in the case of a rapidly rotating curling rock, the velocity of the segment relative to the adjacent film not being in the same direction as the velocity of the segment relative to the solid ice surface.

Moreover, we hypothesize that *rotational motion will cease prior to translational motion* for a cylinder having contact segments as described. The reason we expect this is as follows. For a *rapidly rotating* curling rock, with the thin liquid film being dragged *tangentially* around the rock, *translation*

stops before rotation. For a *slowly rotating* cylinder with *radially* oriented contact segments, we have virtually the opposite situation as compared to the rapidly rotating curling rock, and we therefore expect the opposite physical behaviour, namely, that *rotational motion will stop prior to translational motion*. After we have presented the equations of motion for the cylinder, and also derived the analytical approximations for the translational and rotational speeds as functions of time, we will return to this hypothesis, and the following consequence of the hypothesis. The rotational speed will decrease much more rapidly than the translational speed, and thus the rotational motion will stop prior to the translational motion. In the meantime, we expound upon the physical motion expected.

First consider the case of no rotational motion. Once the cylinder has been released, the relative motion between the radial contact segments and the ice will induce kinetic melting of the ice. The thin liquid film will then be subjected to the adhesive force between the contact segment and the liquid. Some of the liquid will thus be accelerated and will tend to be drawn along with the contact segments. As the cylinder slides, the liquid film beneath it will tend to flow radially along the segments. The liquid closest to a segment will flow fastest, whereas the liquid nearest the ice will exhibit essentially no movement relative to the ice. The main consequence of this is that the velocity of a cylinder's segment relative to the liquid film immediately beneath it will be considerably smaller, and in a different direction, than the velocity of the segment relative to the underlying solid ice surface.

Next consider the case where the cylinder rotates slowly and moves translationally such that $r\omega_0 << v_0$, with v_0 also small enough that the liquid can be dragged along with the contact segment. The ideas of the above paragraph still apply, except we need to include the rotational motion. Consider a given contact segment of the cylinder. We denote the velocity of the contact segment of the cylinder, relative to the solid ice surface, by $\boldsymbol{v}_{\mathrm{c/s}} \equiv \boldsymbol{v}_{\mathrm{s}}$, and the velocity of the segment relative to the adjacent liquid film by $\boldsymbol{v}_{\mathrm{c/liq}} \equiv \boldsymbol{v}_{\mathrm{liq}}$. Given that the cylinder is rotating slowly, the contact segment will still tend to drag some of the liquid film along with it.

As described above, we expect that the adhesion of the liquid film will be such that the liquid will be dragged primarily *along the length* of the contact segment, i.e., radially outward from, or inward toward, the center of the bottom of the cylinder, and almost not at all *perpendicular* to the segment, i.e., perpendicular to the radial direction. The consequence of this is that the velocity $\boldsymbol{v}_{\mathrm{liq}}$ of the segment relative to the adjacent liquid film will be given by

$$\boldsymbol{v}_{\mathrm{liq}} = \epsilon \boldsymbol{v}_{\mathrm{r}} + \boldsymbol{v}_{\mathrm{t}} \tag{1}$$

where $\boldsymbol{v}_{\mathrm{r}}$ and $\boldsymbol{v}_{\mathrm{t}}$ are the *radial* and *tangential* components of the velocity relative to the solid ice surface and $0 < \epsilon < 1$; see Fig. 2.

We emphasize that $\boldsymbol{v}_{\mathrm{liq}}$ and $\boldsymbol{v}_{\mathrm{s}}$ are not in the same direction! We have

$$\boldsymbol{v}_{\mathrm{s}} = \boldsymbol{v}_{\mathrm{trans}} + \boldsymbol{v}_{\mathrm{rot}} \tag{2}$$

where $\boldsymbol{v}_{\mathrm{trans}} \equiv \boldsymbol{v}$ is the translational velocity of the center of mass relative to the ice, and $\boldsymbol{v}_{\mathrm{rot}}$ is the "rotational" velocity of a given contact segment relative to the center of mass, as shown in Fig. 2.

In the case that $0 < \epsilon < 1$ with ϵ small enough, we have that the direction of the force acting on a given portion of the contact segment is opposite in direction to $\boldsymbol{v}_{\mathrm{liq}}$, and not $\boldsymbol{v}_{\mathrm{s}}$, as is clear in Fig. 2. We will show below that the consequence is that the translational motion will continue for a longer time than the rotational motion.

We treat (1) for $\boldsymbol{v}_{\mathrm{liq}}$ as an hypothesis. We will see that the predictions of (1) will be confirmed. In particular, that rotational motion ceases well before translational motion for slowly rotating cylinders having a contact geometry as described above is a prediction of (1) that is confirmed by observation of the motion of a cylinder of the type described. Such agreement thus elevates the proposal to that of a model. We emphasize that, the alternative proposal that $\boldsymbol{v}_{\mathrm{liq}} = \epsilon \boldsymbol{v}_{\mathrm{s}}$ has the consequence that rotational and translational motion of the cylinder cease simultaneously, contrary to what is observed,

Fig. 2. (*a*) The contributions $\boldsymbol{v}_{\rm trans} \equiv \boldsymbol{v}$ and $\boldsymbol{v}_{\rm rot}$ (with $v_{\rm rot} = r\omega$) to the net velocity $\boldsymbol{v}_{\rm s} \equiv \boldsymbol{v}_{\rm s}(\theta)$, relative to the ice, of a contact segment located at an angle θ relative to the x-axis: $\boldsymbol{v}_{\rm s} = \boldsymbol{v} + \boldsymbol{v}_{\rm rot}$. (*b*) The tangential and radial components of $\boldsymbol{v}_{\rm s}$, $\boldsymbol{v}_{\rm t}$ and $\boldsymbol{v}_r$: $\boldsymbol{v}_s = \boldsymbol{v}_t + \boldsymbol{v}_r$. (*c*) The net velocity $\boldsymbol{v}_{\rm liq} \equiv \boldsymbol{v}_{\rm liq}(\theta)$, *relative to the underlying thin liquid film*: $\boldsymbol{v}_{\rm liq} = \epsilon \boldsymbol{v}_{\rm r} + \boldsymbol{v}_{\rm t}$. The figures shown are for a segment located in the first quadrant; similar figures are readily constructed for the other three quadrants. The angle θ in each case is from the x-axis toward the y-axis. Note that the rectangle in parts (*b*) and (*c*) is the same as the one in part (*a*). Also note that the force $\Delta \boldsymbol{F}$ exerted on the segment is in the direction *opposite to* $\boldsymbol{v}_{\rm liq}$, and that this direction is *different than the direction opposite to* $\boldsymbol{v}_s$.

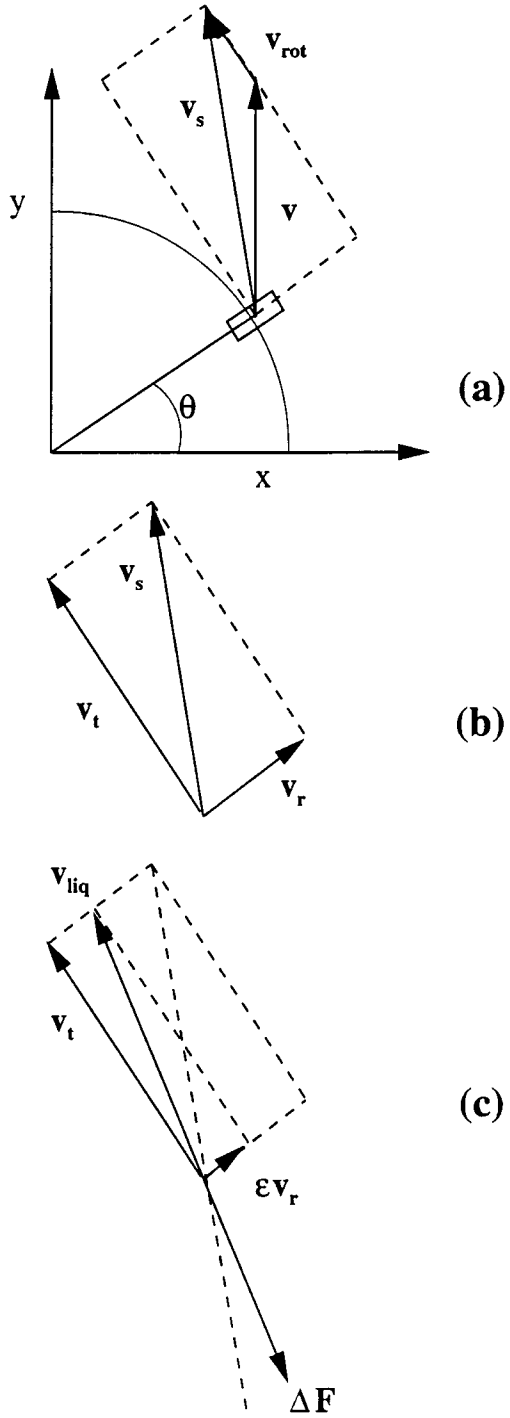

thus rendering this alternative proposal as incorrect. (Extreme exceptional possibilities are discussed later in this paper.)

In summary, our model predicts that the motion of the cylinder over pebbled ice gives kinetic melting and a thin liquid film; the thin film is dragged along the contact segments by adhesion, with the result that, in the case of slow rotation, the forces on the contact segments are *not* opposite to the directions of motion of the contact segments *relative to the solid ice surface*. The consequence is that rotational motion ceases before translational motion.

We tested this prediction by projecting such a cylinder with small initial angular speeds and translational speeds such that $r\omega_0 << v_0$ (typically, $r\omega_0/v_0 \approx 0.1$). We restrict attention to slow speeds because, if the angular and translational speeds are too large, the adhesion between contact segments and the liquid film will not be strong enough to drag much liquid along the segment. We observed that the duration of rotational motion was shorter than that of translational motion, and found that the smaller the ratio $r\omega_0/v_0$, the greater the difference in the times taken for rotation to stop and for translational motion to stop.

4. Equations of motion for the rotating cylinder

We next give the equations that determine the motion of a slowly rotating cylinder. This is a straightforward exercise in determining the net force and torque exerted on the cylinder by the thin film adjacent to the contact segments.

The motion we will investigate is almost straight-line motion: any lateral motion is usually negligible. We therefore focus on the time dependences of the most interesting aspects of the motion, namely, the translational speed $v(t)$ and the angular speed $\omega(t)$.

We choose coordinate axes as follows. The y-axis is in the direction of the velocity of the center of mass of the cylinder, and the x-axis is perpendicular to the velocity. We break up the cylinder into four quadrants, and define θ as the angle from the x-axis toward the y-axis with $0 \leq \theta \leq \pi/2$.

We take the friction exerted on a contact segment of the cylinder to be in the direction opposite to the velocity $\boldsymbol{v}_{\rm liq}(\theta)$ of the segment relative to the adjacent liquid film. The magnitude of the friction is $\Delta F = \mu Mg(\Delta\theta/2\pi)$, where μ is the coefficient of kinetic friction, M is the mass of the cylinder, g is the acceleration due to gravity, and $\Delta\theta = 2\pi/N$, where N is the number of contact segments. (The nonuniformity in the normal force around the cylinder is negligible in our model; the nonuniformity is a consequence of the acceleration due to friction.)

To simplify the treatment, we take the magnitude ΔF of the friction to be approximately constant; i.e., we take μ to be constant. We also take ϵ to be constant. We expect that both ϵ and μ will actually exhibit complicated time dependences. For the purposes of this work, it is unnecessarily complicated to obtain and employ a first-principles derivation of the time-dependent forms of $\epsilon(t)$ and $\mu(t)$. Our focus will be, instead, to take ϵ and μ as effective values that reproduce the principal features of the overall motion. We will see below that this is indeed a reasonable approach, and we will comment on this later in the paper.

By considering each quadrant of the cylinder separately, the following equations for the net force and the net torque on the rock are readily obtained. To simplify the treatment, we approximate the sum over discrete segments by integration over a continuous angle θ. We have

$$F = -\frac{1}{\pi}\mu Mg\int_0^{\pi/2} \mathrm{d}\theta \left[\cos\left(\theta - \tan^{-1}\left[\frac{\epsilon v\sin\theta}{v\cos\theta + r\omega}\right]\right) + \cos\left(\theta - \tan^{-1}\left[\frac{\epsilon v\sin\theta}{v\cos\theta - r\omega}\right]\right)\right] \qquad (3)$$

The equation for the torque is

$$\tau = -\frac{1}{\pi}r\mu Mg\int_0^{\pi/2} \mathrm{d}\theta \left[\cos\left(\tan^{-1}\left[\frac{\epsilon v\sin\theta}{v\cos\theta + r\omega}\right]\right) - \cos\left(\tan^{-1}\left[\frac{\epsilon v\sin\theta}{v\cos\theta - r\omega}\right]\right)\right] \qquad (4)$$

In these equations, $v(t) \equiv v \equiv v_{\rm trans}$ is the instantaneous speed of the center of mass of the cylinder; $\omega(t) \equiv \omega$ is the instantaneous angular speed of the cylinder; and θ in each quadrant is measured from the x-axis toward the y-axis, as shown in Fig. 2.

Figure 2 is presented to assist in understanding the above equations. Figure 2*a* shows the contributions $\boldsymbol{v}_{\rm trans} \equiv \boldsymbol{v}$ and $\boldsymbol{v}_{\rm rot}$ (with $v_{\rm rot} = r\omega$) to the net velocity $\boldsymbol{v}_s \equiv \boldsymbol{v}_s(\theta)$, relative to the ice, of a contact segment located at angle θ; recall that $\boldsymbol{v}_{\rm s} = \boldsymbol{v}_{\rm trans} + \boldsymbol{v}_{\rm rot}$, and recall that the velocity of the center of mass of the cylinder relative to the ice is simply $\boldsymbol{v}_{\rm trans}$. Figure 2*b* shows $\boldsymbol{v}_{\rm s}$ in terms of its tangential component $\boldsymbol{v}_{\rm t}$ and its radial component $\boldsymbol{v}_{\rm r}$: $\boldsymbol{v}_{\rm s} = \boldsymbol{v}_{\rm t} + \boldsymbol{v}_{\rm r}$. Note that $v_{\rm t} = v\cos\theta \pm r\omega$ and $v_{\rm r} = v\sin\theta$. Figure 2*c* shows the velocity, $\boldsymbol{v}_{\rm liq}$, of the contact segment at angle θ, relative to the underlying thin liquid film: $\boldsymbol{v}_{\rm liq} = \epsilon\boldsymbol{v}_{\rm r} + \boldsymbol{v}_{\rm t}$. Also shown in this figure is the force $\Delta\boldsymbol{F}$ exerted on the contact segment. We emphasize that $\Delta\boldsymbol{F}$ is in the direction *opposite to* $\boldsymbol{v}_{\rm liq}$, and that this is *not the same as the direction opposite to* $\boldsymbol{v}_{\rm s}$, as is manifest from Fig. 2.

Similar figures are readily constructed for the other three quadrants of the cylinder. The equations above include the contributions from each of the four quadrants.

The velocity of the cylinder at any time t is readily obtained numerically from the above equations along with $\boldsymbol{F} = M\,{\rm d}\boldsymbol{v}/{\rm d}t$, and initial conditions:

$$v(t) = v_0 + \int_0^t {\rm d}t' a(t') \tag{5}$$

where $a = F/M$ is simply the acceleration of the center of mass. The angular speed ω is given by

$$\omega(t) = \omega_0 + \int_0^t {\rm d}t' \alpha(t') \tag{6}$$

where $\tau \approx \frac{1}{2}MR^2\alpha$ determines the time development of the angular acceleration α of the cylinder; M is the mass of the cylinder, and R is the radius of the cylinder. We point out that the mass of the plate is but a small fraction of the mass of the curling rock. Note that the radial position locating the contact segments, r, has been chosen to be significantly larger than the radius of the cylinder, R: $r \approx 20.0$ cm; $R \approx 14.0$ cm (see Fig. 1). The reason for this will be given after the approximate, analytical expressions are presented. The location $y(t)$ of the center of mass of the cylinder, and the angle $\Delta\theta(t)$ through which the cylinder has rotated since its release, may be obtained by using

$$y(t) = y_0 + \int_0^t {\rm d}t' v(t'), \qquad \Delta\theta(t) = \int_0^t {\rm d}t' \omega(t') \tag{7}$$

The coefficient of friction, μ, may be estimated by direct observation of the sliding cylinder. This would leave ϵ as the single parameter in the problem. Alternatively, if an estimate of ϵ is made, μ may be regarded as the single parameter.

Equations (3)–(6) are readily solved to leading order for the case $r\omega << v$. The result is

$$v(t) = v_0\left(1 - \frac{t}{t_0}\right), \qquad \omega(t) = \omega_0\left(1 - \frac{t}{t_0}\right)^{\phi} \tag{8}$$

with

$$t_0 = \frac{v_0}{\mu g J_0(\epsilon)}, \qquad \phi = \frac{2r^2 J_1(\epsilon)}{R^2 J_0(\epsilon)} \tag{9}$$

where

$$J_0(\epsilon) = \frac{2}{\pi}\int_0^{\pi/2} {\rm d}\theta \cos\left(\tan^{-1}[\epsilon\tan\theta] - \theta\right) \tag{10}$$

and

$$J_1(\epsilon) = \frac{2\epsilon}{\pi}\int_0^{\pi/2} \mathrm{d}\theta \frac{\sin\theta}{\epsilon^2\sin^2\theta + \cos^2\theta}\sin\left(\tan^{-1}[\epsilon\tan\theta]\right)$$

$$= \frac{2\epsilon^2}{\pi}\int_0^{\pi/2} \mathrm{d}\theta \frac{\sin^2\theta}{\left[\epsilon^2\sin^2\theta + \cos^2\theta\right]^{3/2}} \tag{11}$$

If the exponent ϕ in (8) for $\omega(t)$ is greater than one, and large enough, then $\omega(t)/\omega_0$ will go to zero much more quickly than $v(t)/v_0$. (One can easily show that this requires $\phi > 2$ to 2.5.) This can occur, for a given value of ϵ, if the ratio r/R is large enough. This is why we have chosen $r \approx 20.0$ cm, $R \approx 14.0$ cm. We will return to this point when we present our results.

In these approximate, analytical equations, t_0 represents the *approximate* stopping time. It is very important to recognize that this asymptotic form is a good approximation provided $r\omega << v$ and ϵ is not too close to zero; the approximation breaks down as $\epsilon \to 0$.

The exact numerical results shown in the following figures (next section) are compared to these asymptotic forms. We see that these approximations are very good, and we comment on this more fully later.

Having derived these analytical forms for $v(t)$ and $\omega(t)$, we can see that our hypothesis, i.e., that rotational motion will cease well before translational motion, emerges as a consequence of (8) and (9). If $\phi > 1$ and is large enough (e.g., $\phi > 3$), $\omega(t)/\omega_0$ will go to zero much more rapidly than $v(t)/v_0$. In our previous work on slowly rotating curling rocks (i.e., $r\omega << v$), we derived asymptotic forms for $v(t)$ and $\omega(t)$; those expressions were of the same forms as (8)–(11), but with $1/\epsilon$ replacing ϵ in these equations (see ref. 2 for details). As such, it is natural to ask if one could observe rotational motion stopping prior to translational motion, *for a curling rock*. Given the values of r and R for a curling rock, one easily confirms that $\phi < 1$. What would happen if the contact annulus was replaced by a contact annulus with a much larger value of r?

In Fig. 3 we compare $\omega(t)/\omega_0$ for a modified curling rock, with $r = 0.2$ m, to $\omega(t)/\omega_0$ for a cylinder having the contact geometry shown in Fig. 1, also with $r = 0.2$ m. The figure clearly shows that the cylinder will stop rotating well before translation ceases, while the "modified curling rock" will have both rotation and translation stop simultaneously. This is why we have constructed the cylinder and examined its motion. For completeness, we do wish to point out that it is possible for rotation to stop before translation, even if the contact geometry is a thin circular annulus: one requires $\epsilon \approx 1$ and (or) a fairly large value of r (e.g., as in Fig. 3, but with $\epsilon \geq 0.1$ and $r \geq 0.3$ m).

5. Results

We have done several numerical runs in order to explore the qualitative and quantitative features of the motion of cylinders having the contact geometry shown in Fig. 1.

We show the principal features of the ϵ–dependence of the motion in Figs. 4*a* and 4*b*, the r-dependence in Figs. 5*a* and 5*b*, and in Fig. 6 the dependence on the ratio $s_0 \equiv r\omega_0/v_0$. In all of these figures, we have $R = 0.14$ m, and we choose $\mu = 0.05$. In Figs. 4 and 5 we also have $v_0 = 1.5$ m s^{-1} and $\omega_0 = 0.75$ s^{-1}.

From Fig. 4*a*, where $\epsilon = 0.1$, we see clearly that the model predicts that rotation stops well before translation; the duration of rotation is $t_{\mathrm{rot}} < 3.2$ s, while translational motion continues up to $t_{\mathrm{trans}} \approx 3.8$ s. In Fig. 4*b*, where $\epsilon = 1$, we have both rotation and translation stopping at approximately the same time: $t_{\mathrm{rot}} \approx t_{\mathrm{trans}} \approx 3.0$ s. In both figures, $r = 0.20$ m. Similar figures for other values of ϵ show two principal features: (1) the total duration of all motion decreases as ϵ increases, and (2) the difference between t_{rot} and t_{trans} decreases with ϵ.

Fig. 3. Plots of $\omega(t)/\omega_0$ (continuous-line curves) and $v(t)/v_0$ (broken-line curves) as functions of time t (in seconds) for $\epsilon = 0.1$ for a cylinder with the contact geometry of Fig. 1 (lower continuous-line curve) and for a curling rock modified so that its contact annulus has radius r (upper continuous-line curve). While $v(t)$ is the same for the two cases, the $\omega(t)$ curves are distinct. The "modified curling rock" would have both rotation and translation cease simultaneously, while the segmented cylinder will stop rotating well before translational motion ceases. In both cases, $v_0 = 1.5$ m s^{-1}, $\omega_0 = 0.75$ s^{-1}, $\mu = 0.05$, $r = 0.20$ m, and $R = 0.14$ m. Note also the excellent agreement between the analytical curves (lighter lines) and numerical curves (heavier lines): the analytical and numerical curves are so close as to be virtually indistinguishable, i.e., the curves essentially lie on top of one another.

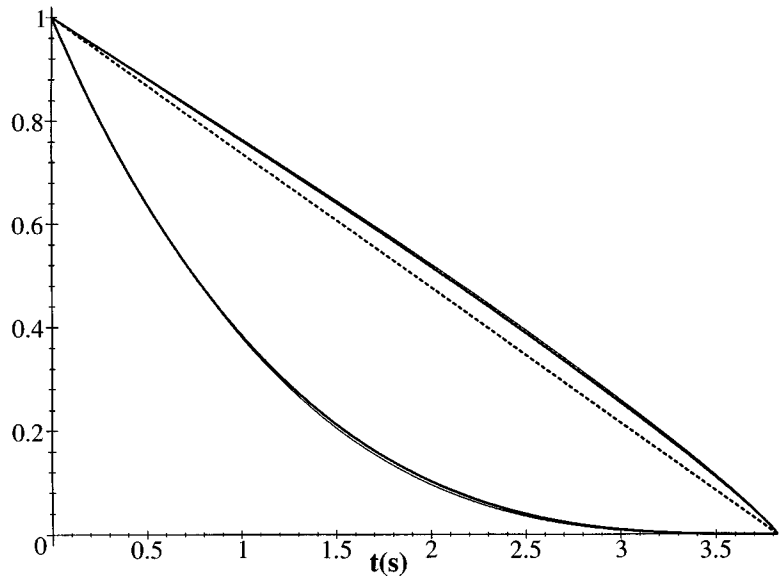

Figures 5*a* and 5*b* compare the motions for $r > R$ and $r < R$. In Fig. 5*a*, where $r = 0.3$ m, the rotation stops well before translation: $t_{\text{rot}} < 2.1$ s, while $t_{\text{trans}} \approx 3.8$ s. In Fig. 5*b*, where $r = 0.0625$ m (the radius of the contact annulus of a curling rock), the rotation and translation switch roles: the $v(t)/v_0$ curve, while still linear in t, goes to zero faster than the $\omega(t)/\omega_0$ curve. Note the difference in the $\omega(t)/\omega_0$ curves in Figs. 5*a* and 5*b*. For this smaller value of r, $t_{\text{rot}} = t_{\text{trans}}$. Comparing Figs. 4*a* and 5*a* we see that, for $r > R$, t_{rot} decreases as r increases, while t_{trans} is virtually constant.

For large values of r, even with $\epsilon = 1$, one can have rotational motion stop well before translational motion. For example, with $v_0 = 1.5$ m s^{-1}, $\omega_0 = 0.75$ s^{-1}, $\mu = 0.05$, $R = 0.14$ m, and $\epsilon = 1$, taking $r = 1.0$ m one finds that rotation stops after only about 0.35 s, while translational motion stops at about 3.06 s! This occurs because the exponent ϕ is very large in this example. Note, however, that this is a rather extreme, exceptional example.

Note that all of these features can be understood from the approximate analytical forms given in (8)–(11), and also that these approximations are, in almost all the figures in this paper, virtually indistinguishable from the exact (numerical) curves in these figures. Also note that it is straightforward to show that the analytical approximation breaks down, as expected, as $\epsilon \to 0$.

Figures 6 and 4*a* show the dependence of the motion on $s_0 \equiv r\omega_0/v_0$. The principal changes, as s_0 goes from 0.1 (Fig. 4*a*, with $\omega_0 = 0.75$ s^{-1}) to 1 (Fig. 6, with $\omega_0 = 7.5$ s^{-1}), are as follows. The

Fig. 4. Plots of $\omega(t)/\omega_0$ (continuous-line curves) and $v(t)/v_0$ (broken-line curves) as functions of time t (in seconds) for (*a*) $\epsilon = 0.1$, and (*b*) $\epsilon = 1$. In both figures, $v_0 = 1.5$ m s^{-1}, $\omega_0 = 0.75$ s^{-1}, $\mu = 0.05$, $r = 0.20$ m, and $R = 0.14$ m. Note the excellent agreement between the analytical curves (lighter lines) and numerical curves (heavier lines).

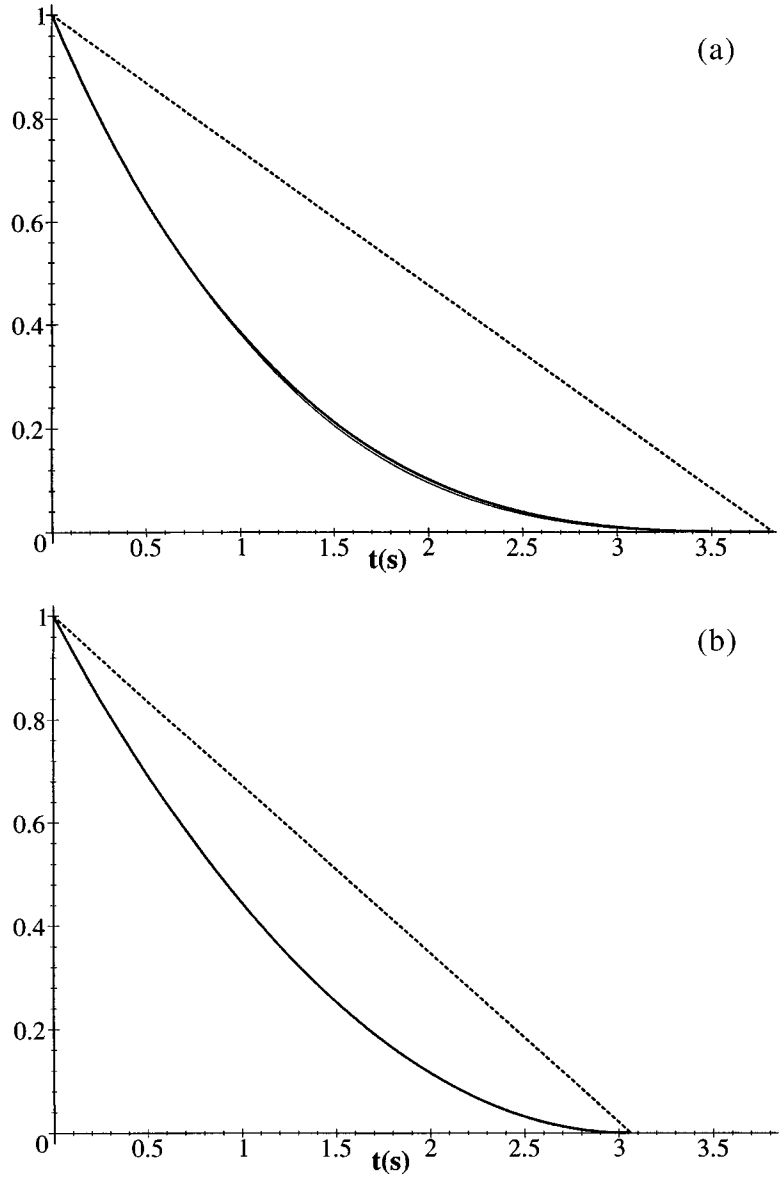

duration of translational motion increases from $t_{\text{trans}} \approx 3.8$ s for $s_0 = 0.1$ to $t_{\text{trans}} \approx 4.1$ s for $s_0 = 1$. The rotational motion, however, ensues for $t_{\text{rot}} < 3.2$ s, independent of the value of s_0. Indeed, the curves for $\omega(t)/\omega_0$ are virtually identical in Figs. 4*a* and 6. Notice also that the analytical approximation for $\omega(t)/\omega_0$ is extremely good, even for $s_0 = 1$! The approximation for $v(t)/v_0$ is not as good; while it is still linear at $s_0 = 1$, the approximate stopping time of 3.8 s is less than the exact value of 4.1 s.

Fig. 5. Plots of $\omega(t)/\omega_0$ (continuous-line curves) and $v(t)/v_0$ (broken-line curves) as functions of time t (in seconds) for (*a*) $r = 0.3$ m, and (*b*) $r = 0.0625$ m. In both figures, $v_0 = 1.5$ m s^{-1}, $\omega_0 = 0.75$ s^{-1}, $\mu = 0.05$, $R = 0.14$ m, and $\epsilon = 0.1$. Note the excellent agreement between the analytical curves (lighter lines) and numerical curves (heavier lines).

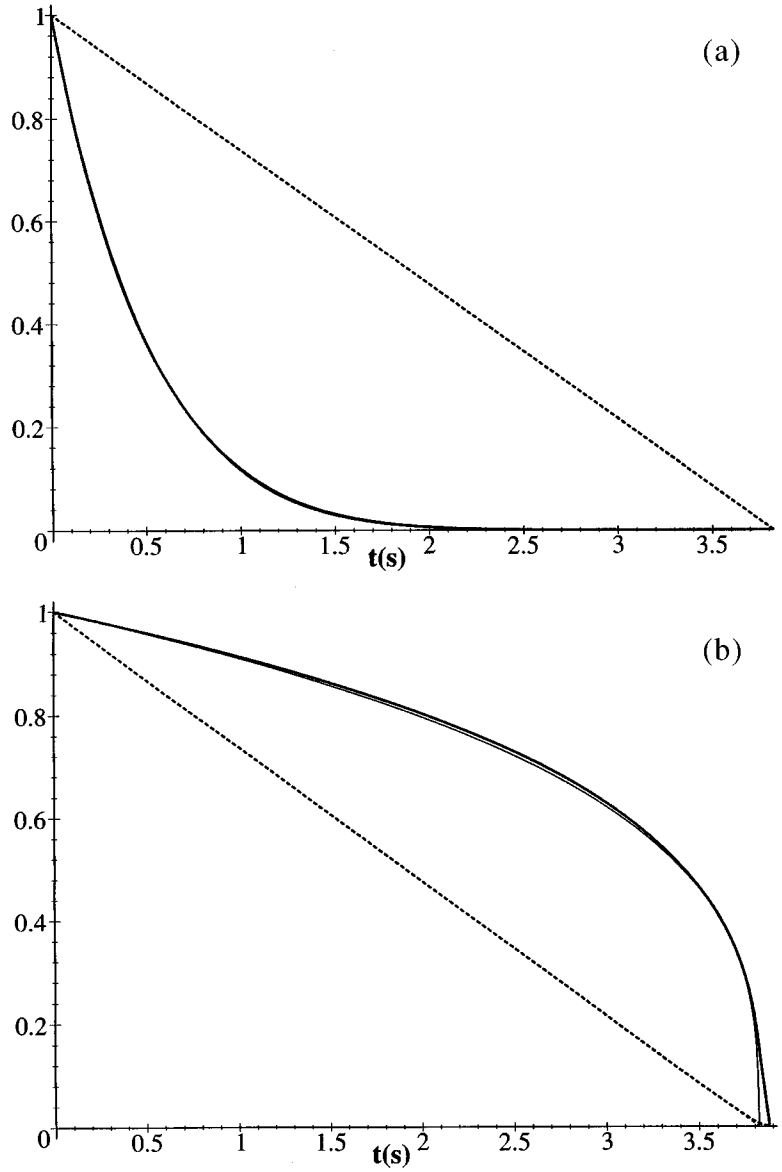

Using the features of the motion revealed by Figs. 4–6, we next compare our model with observed motions of the actual cylinder. Before doing so, we must discuss two physical features associated with the cessation of motion of the cylinder.

We first consider a key aspect of the cessation of rotational motion. Recall that curling ice is not perfectly flat: it is pebbled, having rounded protrusions and accompanying valleys. Consequently, as

Fig. 6. Plots of $\omega(t)/\omega_0$ (continuous-line curves) and $v(t)/v_0$ (broken-line curves) as functions of time t (in seconds) for $s_0 \equiv r\omega_0/v_0$=1, using the values: $v_0 = 1.5$ m s^{-1}, $\omega_0 = 7.5$ s^{-1}, $\mu = 0.05$, $r = 0.20$ m, $R = 0.14$ m, and $\epsilon = 0.1$. Note the excellent agreement between the analytical curve (lighter line) and numerical curve (heavier line) for $\omega(t)/\omega_0$.

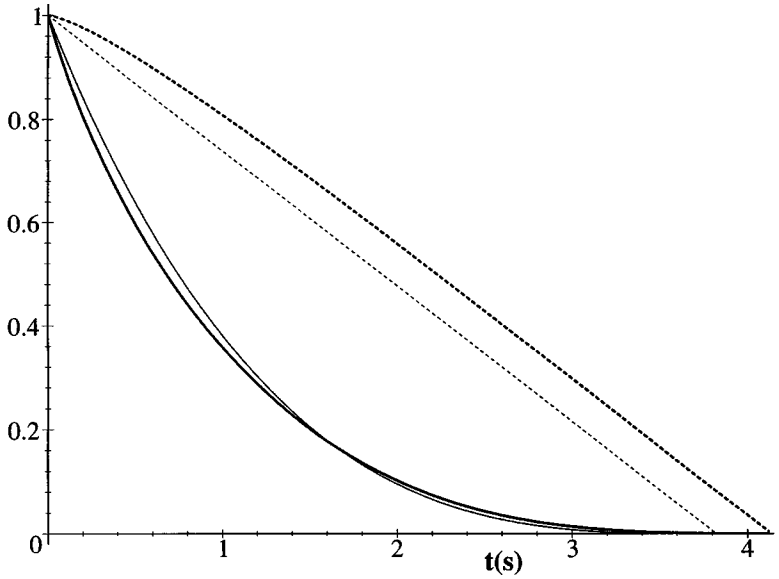

the cylinder moves over the ice, its center of mass will experience small changes in its vertical position, and thus also in its gravitational potential energy. There is a minimum rotational speed which the cylinder must have if one side of the cylinder is to be able to rise a vertical distance $h_{\rm peb}$ higher than the opposite side. A simple calculation gives the following estimate for the minimum rotational speed: $\omega_{\rm min} \approx (gh_{\rm peb})^{1/2}/R$. For example, for $h_{\rm peb} \approx 0.02$ mm, $\omega_{\rm min} \approx 0.1$ s^{-1}. Recall that $h_{\rm peb}$ is the scale over which the vertical position of the rock's center of mass varies, and is not the size of the pebbles themselves.

The important consequence of this minimum rotational speed is that a real cylinder of the type under question will stop somewhat suddenly, albeit at a rather slow rotational speed. This is especially important for the case of slow rotation, where $v(t)$ drops much more slowly to zero than $\omega(t)$. Recall that this behaviour is associated with ϕ being sufficiently greater than one (see (8) and (9)). The result of these different rates of decrease is that $t_{\rm rot}$ is not only *smaller* than $t_{\rm trans}$, but is *considerably* smaller than $t_{\rm trans}$, for the slowly rotating cylinder; after the cylinder has stopped rotating, its translational motion will therefore continue for an appreciable time.

The translational motion of the cylinder will also stop somewhat suddenly, again at a rather low speed. The physical reason for this is that there is a minimum speed needed to induce kinetic melting of the ice. Once the cylinder's translational speed drops down to this minimum, all motion will cease rather quickly. Although this minimum speed is so small as to be negligible in this paper ($v_{\rm min} \approx 2$ cm s^{-1}), we have discussed this point for the sake of completeness.

In Table 1, we compare observed values with the values given by the model for 2 different cases. The values of μ are different than for curling rocks because the contact segments are metal while curling rocks are granite. Similarly, the value of ϵ here is different than that used for curling rocks; more specifically, because metal–liquid adhesion will certainly be different that granite–liquid adhesion, different values of ϵ are expected in the two different cases. The observed values were obtained by videotaping the

Table 1. This table gives the initial speed, v_0, initial angular speed, ω_0, the ratio $s_0 \equiv v_0/(r\omega_0)$, and the effective coefficient of kinetic friction, μ, for two observed shots. The observed and calculated values of the duration of translational motion, $t_{\rm trans}^{\rm obs}$ and $t_{\rm trans}^{\rm calc}$, the duration of rotational motion, $t_{\rm rot}^{\rm obs}$ and $t_{\rm rot}^{\rm calc}$, the total distance traveled, $y_{\rm tot}^{\rm obs}$ and $y_{\rm tot}^{\rm calc}$, and the total angle of the rotation, $\Delta\theta_{\rm tot}^{\rm obs}$ and $\Delta\theta_{\rm tot}^{\rm calc}$, are also compared. The parameter ϵ is 0.075 in both cases.

Shot	v_0 (m s^{-1})	ω_0 (s^{-1})	s_0	μ	$t_{\rm trans}^{\rm obs}$ (s)	$t_{\rm trans}^{\rm calc}$ (s)	$t_{\rm rot}^{\rm obs}$ (s)	$t_{\rm rot}^{\rm calc}$ (s)	$y_{\rm tot}^{\rm obs}$ (m)	$y_{\rm tot}^{\rm calc}$ (m)	$\Delta\theta_{\rm tot}^{\rm obs}$	$\Delta\theta_{\rm tot}^{\rm calc}$
(a)	1.7	1.25	0.15	0.040	5.5	5.6	3.0	2.8	4.9	4.8	1.6	1.6
(b)	1.5	1.8	0.24	0.045	4.2	4.2	2.2	2.2	3.5	3.3	1.8	1.8

Fig. 7. Theoretical results and observed values for shot (b) in Table 1. The fraction of the angle of rotation, $\Delta\theta(t)/\Delta\theta(t_0)$ (continuous-line curve, filled squares), and the fraction of the distance traveled, $y(t)/y(t_0)$ (broken-line curve, open squares), are plotted as a function of the fraction of the total time of translational motion, t/t_0; $\Delta\theta(t_0)$ is the total angle through which the cylinder rotated, $y(t_0)$ is the total distance traveled, and t_0 is the total time of translational motion. The agreement between theoretical and observed values is rather good. Note also that the cessation of rotational motion prior to translation is manifest. The cross (+) on the continuous-line curve indicates the time at which $\omega = \omega_{min} = 0.1$ s^{-1}; i.e., cessation of rotation.

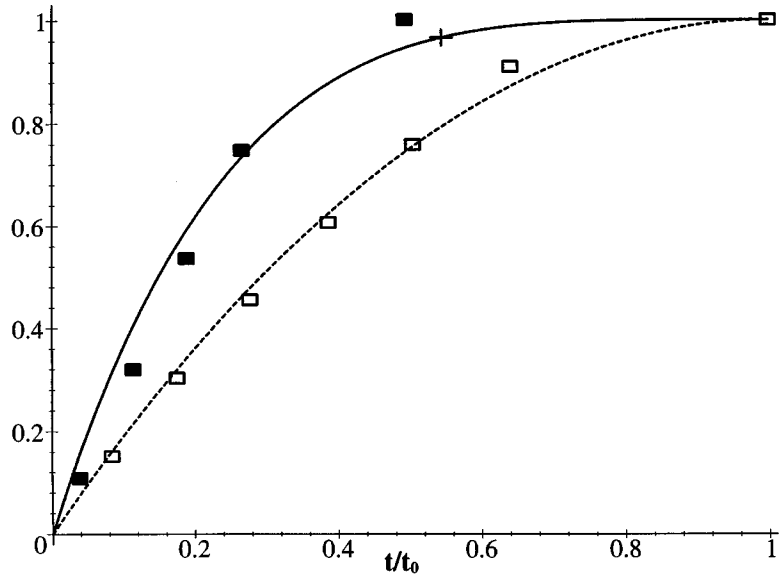

cylinder's motion. Errors in the observed values are at most of order ± 1 in the last digit given. The primary source of error was the time interval (1/60 s) between successive frames of the videotape. Rotational motion was taken to stop once ω had dropped to $\omega_{\rm min} \approx 0.1$ s^{-1}.

In Fig. 7 we compare theoretical results for, and observed values of $\Delta\theta(t)/\Delta\theta(t_0)$ (continuous-line curve, filled squares) and $y(t)/y(t_0)$ (broken-line curve, open squares) for shot (b) in Table 1; $\Delta\theta(t_0)$ denotes the total angle through which the cylinder rotated, $y(t_0)$ is the total distance traveled, and t_0 is the total time of translational motion. The agreement between the observed values, and the values

obtained from the model, is rather good, especially upon considering the approximations made in our model, and the complicated nature of the motion studied; the main approximations are replacing the summation over discrete segments by integration over a continuous angle, and treating the complicated time dependences of $\mu(t)$ and $\epsilon(t)$ by choosing effective, constant values for μ and ϵ. The theoretical curves in Fig. 7 were generated using (7)–(11) and the values in Table 1.

We are quite satisfied that the model, and the underlying ideas, have been shown by this comparison to observed motions to be most promising.

6. Discussion and conclusion

We conclude that the essential ideas in this manuscript explain the motion of a slowly rotating cylinder having radial contact segments sliding over pebbled ice. We emphasize that the results for $v(t)$ and $\omega(t)$ in our model simulations exhibit the correct *qualitative* motion as well as good *quantitative* results.

Such slowly rotating cylinders are observed to stop rotating long before they stop moving translationally; our model successfully accounts for this rather novel feature of the motion of these cylinders.

We point out that other models appear to be unable to explain the motion observed and modeled here. One example is a model proposing that the lateral motion of slowly rotating curling rocks results as a consequence of the nonuniform pressure distribution around the contact annulus, the leading semicircle being subjected to a higher pressure than the trailing semicircle to counteract the lateral torque caused by friction [4]. The main idea in ref. 4 is that the higher leading pressure results in lower friction. In this model, the frictional force exerted on any contact segment of the cylinder would be opposite in direction to the velocity relative to the ice, which thus requires the translational and rotational motions to stop at the same time, contrary to what is actually observed. Another publication [5] considers a "left–right" asymmetry. As has been convincingly demonstrated in ref. 3, the approach taken in ref. 5 calls for unreasonable transverse forces on curling rocks, and, further, makes predictions of motions of curling rocks that are in disagreement with observed motions of actual curling rocks. Since that approach fails to explain why curling rocks curl, it is not appropriate to consider it any further. That a left–right asymmetry cannot account for lateral motion of a curling rock was previously shown in ref. 6.

As stated above, our work agrees rather well with the observed behaviours of slowly or rapidly rotating curling rocks. We emphasize that our idea of the existence of the liquid film and its tendency to be drawn around the rock is crucial for explaining the phenomenon of translational motion ceasing prior to rotational motion in the case of rapidly rotating curling rocks. Our model thus successfully accounts for the cessation of translational motion well before that of rotational motion for rapidly rotating curling rocks.

In this paper we have seen that the same idea, applied to cylinders having a very different contact geometry, explains why such cylinders stop rotating prior to translational motion ceasing. Such motion is observed for real cylinders having the contact geometry examined in this paper.

The work of this and our previous papers [1,2] combine to account both qualitatively and quantitatively for several aspects of the observed motions of real curling rocks, both slowly rotating and rapidly rotating, as well as cylinders of the same size and shape as curling rocks, but with a very different contact geometry.

In view of these agreements between observed motions of curling rocks, cylinders of the type studied in this paper, and the motions given by our model, we conclude that our model presents a reasonable picture of the underlying physics of the motions of curling rocks.

Acknowledgements

We thank the Prince George Golf and Curling Club (PGGCC) for the use of their facilities, and we thank Mr. Murry Kutyn (Head Ice Technician at PGGCC) for much help and useful information. We

appreciate the support of Educational and Media Services of UNBC, and we particularly thank Mr. Andrew Zand, for enabling us to videotape motions of the cylinders. We thank Mr. Mark Pow for constructing the housing, plate, and contact segments used to construct the cylinders. This work was supported financially by the Natural Sciences and Engineering Research Council of Canada.

References

1. M.R.A. Shegelski, R. Niebergall, and M.A. Walton. Can. J. Phys. **74**, 663 (1996).
2. M.R.A. Shegelski and R. Niebergall. Aust. J. Phys. **52**, 1025 (1999).
3. M.R.A. Shegelski and M. Reid. Can. J. Phys. **77**, 903 (1999).
4. G.W. Johnston. Can. Aeron. Space J. **27**, 144 (1981).
5. M. Denny. Can. J. Phys. **76**, 295 (1998).
6. M.R.A. Shegelski, R. Niebergall, and M.A. Walton. Phys. World, **10**(6), 19 (1997).